Contents lists available at SCCE

Journal of Soft Computing in Civil Engineering

Journal homepage: www.jsoftcivil.com

Structural Optimization of Concrete Volume for Machine Foundation Using Genetic Algorithms

M.A. Lopes[1], F.J.C.P. Soeiro[2], J.G. Santos da Silva[3*]

1 D.Sc. Student, Mechanical Engineering Postgraduate Program (PPGEM), State University of Rio de Janeiro (UERJ), Rio de Janeiro/RJ, Brazil

2 Professor, Mechanical Engineering Postgraduate Program (PPGEM), State University of Rio de Janeiro (UERJ), Rio de Janeiro/RJ, Brazil

3 Professor, Civil Engineering Postgraduate Program (PGECIV), State University of Rio de Janeiro (UERJ), Rio de Janeiro/RJ, Brazil

Corresponding author: *matheus.lopes1@hotmail.com*

https://doi.org/10.22115/SCCE.2019.203066.1129

ARTICLE INFO

Article history:
Received: 27 September 2019
Revised: 24 November 2019
Accepted: 26 November 2019

Keywords:
Structural optimization;
Genetic algorithms;
Finite element method;
Dynamic analysis;
Concrete foundation.

ABSTRACT

This research work aims to optimize a concrete foundation designed to support a high-capacity motor-driven compressor. The structure has plane dimensions of approximately 15 m × 11 m and a height of 1.5 m. The concrete block is to be supported by 20 concrete piles approximately 8.5 m in length and 0.5 m in diameter. The investigated structural system is subjected to deterministic dynamic loadings due to the nature of the equipment supported by the concrete foundation. The main objective of the optimization is to reduce the structural volume through the analysis of its dynamic response, in order to minimize the cost of the concrete volume. In this research work, Genetic Algorithms (GAs) are used through an appropriate interface between ANSYS and MATLAB software. The results of this study show that through the GAs it is possible to achieve a considerable volume reduction with respect to the original volume of concrete used in the design of the foundations structural system.

How to cite this article: Lopes MA, Pires Soeiro, FJCP, Santos da Silva, JG. Structural optimization of concrete volume for machine foundation using genetic algorithms. J Soft Comput Civ Eng 2019;3(3):62–81. https://doi.org/10.22115/scce.2019.203066.1129.

1. Introduction

The design and prediction of the behavior of a structure subject to static loadings is a regular task for engineers in charge of projects. However, when dynamic loadings are present in the analyses, this task turns out to be considerably more complex. The design of foundations for dynamic equipment requires the responsible engineer to have some knowledge of dynamic analyses; in addition, to find the best design, optimization techniques can be employed, leading to a lower-cost project [1–3].

Genetic Algorithms (GAs), presented by Holland [4] in 1975, are optimization techniques inspired by Darwin's theory of evolution whose main characteristics are based on the principles of survival of the fittest individual and adaptation. Since then, the fields of application of GAs have been investigated by authors and some varieties of the algorithm have been developed. The improved augmented Lagrangian GA was presented by Adeli [5] as a robust hybrid algorithm for optimization of space structures using the augmented Lagrangian method and, in comparison with the penalty-function-based GA, only a few additional simple function evaluations are needed. In addition, hybrid algorithms of GA with a fuzzy system [6] and with a neural network [7] and elitist GA [8] have been presented as varieties of GAs.

GAs can be applied to a very large variety of problems and, in engineering, their application in structural optimization has gained space. Tayşi [9] used GA to minimize the weight and strain energy of arch structures subjected to constraints on stress, displacement, and weight responses and found that GAs are reliable and provide an efficient way of finding the optimum shapes for variable-curve beams and arches. Vasudev [10] applied GA to optimize a submarine hull shape, which involved maximization of the volume and minimization of the hydrodynamic drag. Rajeev and Krishnamoorthy [11] studied GAs in discrete structural optimization of trusses and found out that GAs are suitable for structural optimization since they handle discrete variables efficiently. Hajela and Lee [12] investigated the application of GA in topological optimization problems and applied its techniques to trusses for stress, buckling, and displacement constraints, showing that the genetic search procedure is a good exploratory tool to evaluate topologies in a discontinuous design space. Camp et al. [13] studied the GA for discrete optimization of two-dimensional structures, applying the method to a one-bay eight-story frame and a three-bay three-story frame, and concluded that GA can handle discrete design variables effectively, making it a practical approach to structural design. Hosseini [14] evaluated the use of GA on artificial neural network training for prediction of the shear capacity of reinforced concrete beams, strengthened with side-bonded fibre reinforced polymer, concluding that it can be used predict the shear capacity. Tazou et al. [15] developed a properly interface between Matlab and ANSYS software to perform a structural optimization of recycled thermoplastic plate based on GA, aiming the minimization of the Von Mises equivalent stress, which led to a design configuration suitable for the load case studied. Karanjule et al. [16] used GA to optimize the process parameters of cold drawing for seamless tubes, in order to minimize the springback (elastic strain recovery after load removal) and obtained results that improved the dimensional tolerances of theses tubes.

The present research work has as its main focus the optimization of a structure designed to support a high-capacity motor-driven compressor. The structural system is located at an industrial plant and consists of a concrete foundation with plane dimensions of approximately 15 m × 11 m and a height of 1.5 m. The structural optimization aims to minimize the cost of the concrete volume of the foundation, considering its dynamic responses when subjected to dynamic loadings from the motor-compressor assembly. The problem of study is to evaluate the use of GA to optimize structures subjected to dynamic loadings, with a properly structural finite element analyses interface in order to reduce its cost. Its significance focuses on demonstrate the versatility of the method in order to optmize engineering problems.

For the optimization, a GA was applied using MATLAB R2015b software, while ANSYS software was used to perform the finite element analyses with the aim of obtaining the dynamic responses of the foundation in peaks of displacements, velocities, accelerations, and natural frequencies. The design recommendations from the ACI-351, DIN-4024-1/2, ISO 2372, ISO 2631-1/2, Brazilian NR-15, and Petrobras N-1848 standards were used as the constraints for the optimization [17–24]. These standards define some concepts and requirements for the safe operation of the equipment, human comfort, and other structural design criteria.

The present study yielded results that demonstrate that advanced optimization techniques can be used as auxiliary tools in structural design projects. In addition, the GA has been shown to be suitable for structural optimization applications as in the real case study presented in this paper, which shows a significant reduction in structural volume compared to the original volume.

2. Optimization modelling

The structural optimization was performed by the MATLAB software, which employed a Genetic Algorithm (GA) to minimize the structural volume of the concrete foundation. As the objective function, the volume $V(X)$ was defined in Eq. 1 in terms of three design variables, x_1, x_2 and x_3. The design variables represent the heights of the concrete blocks and its constant coefficients (152.985; 17.460; and 5.04 m²) represent the areas. The constant value of 0.825 m³ represents the fixed volume of two small pedestals that does not vary along the optimization.

$$V(X) = V(x_1, x_2, x_3) = 152.985 \cdot x_1 + 17.466 \cdot x_2 + 5.04 \cdot x_3 + 0.825\ m^3 \tag{1}$$

The nonlinear constraints for the optimization problem were defined from the standard recommendations in terms of maximum displacements, velocities, and accelerations at selected points of the structure (represented by nodes of the finite element model) and in terms of its natural frequencies. The constraints of displacements, velocities, and natural frequencies concern the safe operation of the equipment supported by the concrete foundation and were defined in terms of the limits established by the ISO 2372 [20] and DIN 4024 [18,19] international standards, as expressed by Eqs. 2 to 4. Acceleration constraints concern the comfort of the people who transit in the equipment area and were defined in terms of the limits established by the ISO 2631 [21,22] international standard, which can be observed in Eq. 5. All the data used in the constraints in Eqs. 2 to 5 were obtained from the finite element analyses for every individual created by the GA. Equation 2 defines that the natural frequencies of each vibration mode (f_{ni}) should have a minimum difference of 10% from the equipment excitation frequency (f_f), and Eqs. 3 to 5 establish the upper limits for the displacements, velocities, and accelerations.

$$0{,}1 - \left|\frac{f_f - f_{ni}}{f_f}\right| \leq 0 \qquad i = 1{,}2{,}\ldots{,}6. \tag{2}$$

$$[Maximun\ nodal\ velocities]_j - 2{,}8\frac{mm}{s} \leq 0 \quad j = 1{,}2{,}\ldots{,}16\ nodes. \tag{3}$$

$$[Maximum\ nodal\ displacements]_k - 20\ \mu m \leq 0 \quad k = 1{,}2{,}\ldots{,}16\ nodes \tag{4}$$

$$[Maximum\ nodal\ acceleration]_l - 1\ m/s^2 \leq 0 \quad l = 1{,}2{,}\ldots{,}9\ nodes \tag{5}$$

Furthermore, the constraints of the upper and lower bounds have been defined as shown in Eqs. 6 to 8. These boundary constraints represent the design space in which the design variables can vary. Another design variable constraint concerns the heights of the pedestals on which the compressor and motor are mounted and guarantee that the engine is always higher than the compressor, represented in Eq. 9.

$$0.6\ \text{m} \geq \text{x}_1 \geq 1.50\ \text{m} \tag{6}$$

$$2.0\ \text{m} \geq \text{x}_2 \geq 3.84\ \text{m} \tag{7}$$

$$1.5\ \text{m} \geq \text{x}_3 \geq 2.65\ \text{m} \tag{8}$$

$$\text{x}_3 - \text{x}_2 \leq 0 \tag{9}$$

The GA used for the optimization uses the Augmented Lagrangian Genetic Algorithm (ALGA) to solve the nonlinear constraint optimization problem. The optimization problem solved by the ALGA was set in Eqs. 10 to 12.

$$\text{Minimize } V(X) \tag{10}$$

Such that:

$$c_i(X) \leq 0, \quad m = 1{,}2 \ldots 4 \tag{11}$$

$$LB \leq X \leq UB \tag{12}$$

where $c_i(X)$ represents the nonlinear inequality constraints and LB and UB represent the constraints of the lower and upper bounds, respectively. A subproblem was formulated by combining the objective and nonlinear constraint functions using the Lagrangian parameters. The subproblem formulation $\emptyset$ was defined as shown in Eq. 13.

$$\emptyset(X, \lambda, s) = V(X) - \sum_{m=1}^{4} \lambda_i s_i \log(s_i - c_i(X)). \tag{13}$$

where $X = (x_1, x_2, x_3)$ is the vector of design variables, the components λ_i of the λ vector are nonnegative and are known as Lagrange multiplier estimates, and the elements s_i of the vector s

are nonnegative shifts. The ALGA transforms the nonlinear constrained optimization problem into an unconstrained optimization subproblem where the function to be minimized is represented in Eq. 13; when this subproblem is minimized while satisfying feasible conditions, the Lagrangian estimates are updated.

3. Structural model

The structure that is the focus of this study is a concrete foundation built in an industrial plant at Ouro Branco/MG Brazil. This foundation was designed to support a high-capacity motor-driven compressor and consists of a reinforced concrete block supported by 20 concrete piles 0.50 m in diameter and 8.50 m in length. The concrete block has plane dimensions of approximately 15 m × 11 m and a height of 1.5 m. The engine is supported by a concrete pedestal with dimensions of 5.55 m × 3.15m with a height of 3.84 m and the compressor is supported by two concrete pedestals with dimensions of 2.40 m × 1.50 m and 2.40 m × 0.60 m, both 2.66 m in height. The concrete used to build the foundation block has a Young's modulus of 26 GPa while the concrete used for the piles has an Young's modulus of 21 GPa (Table 1). Figures 1 to 5 present some illustrations of the concrete foundation. The blue marks in Figure 2 represent the location of the concrete piles, the red details in Figures 3 and 5 represent the concrete pedestals where the compressor is supported and its fixation bolts, and the orange details in Figures 3 and 4 represent the concrete pedestals where the engine is mounted and its fixation bolts.

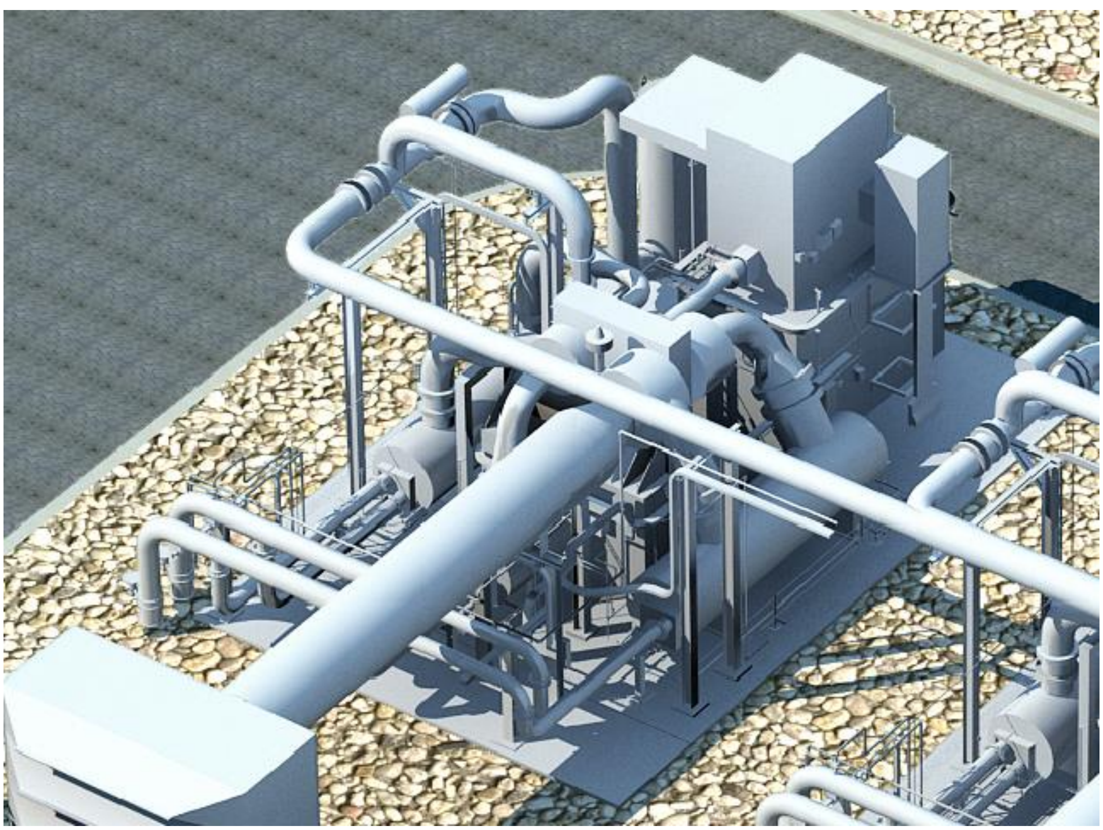

Fig. 1. Concrete foundation and equipment illustration.

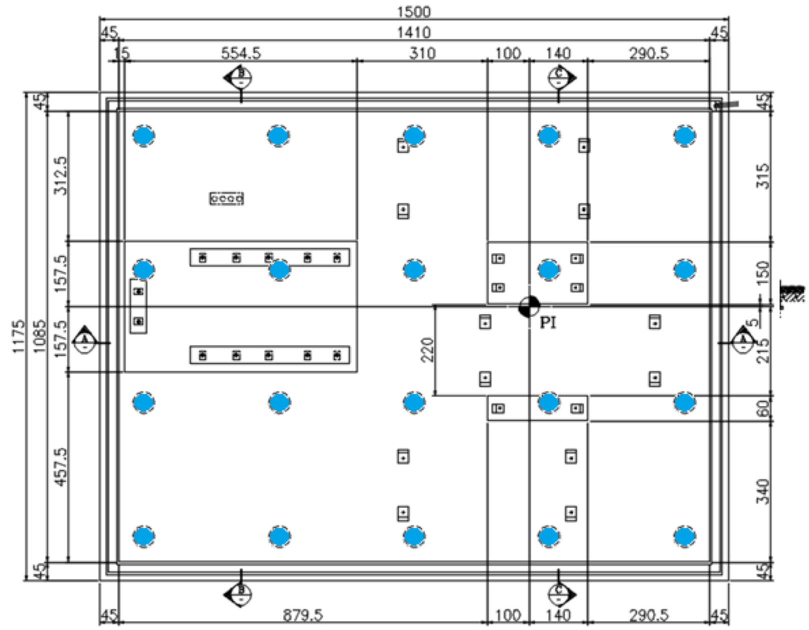

Fig. 2. Plan view from the concrete foundation and piles (dimensions in centimeters).

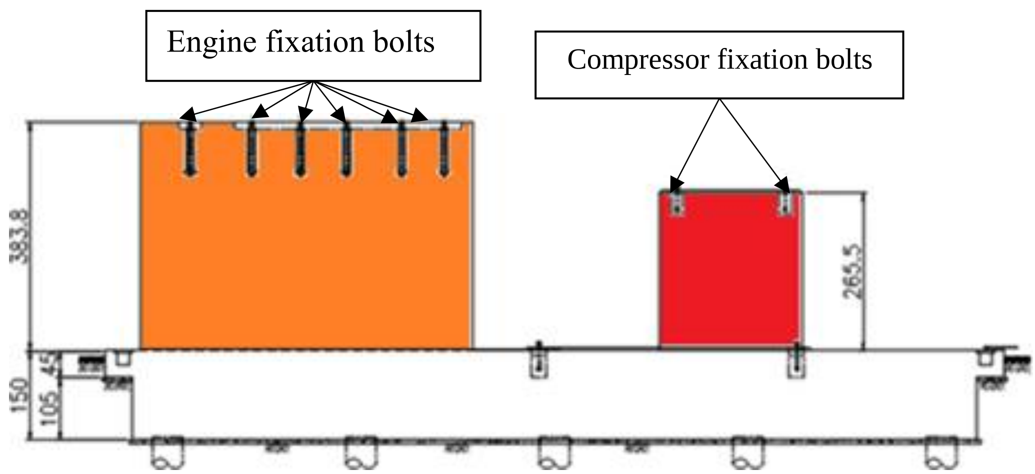

Fig. 3. A-A View from de concrete foundation (dimensions in centimeters).

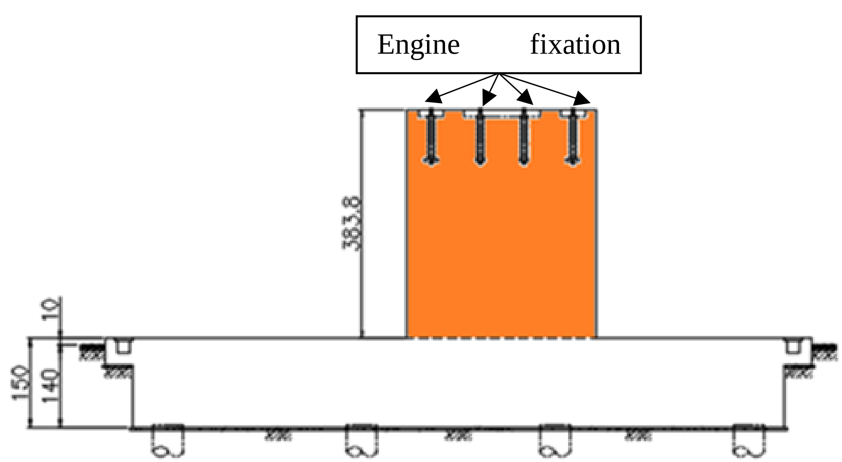

Fig. 4. B-B View from de concrete foundation (dimensions in centimeters).

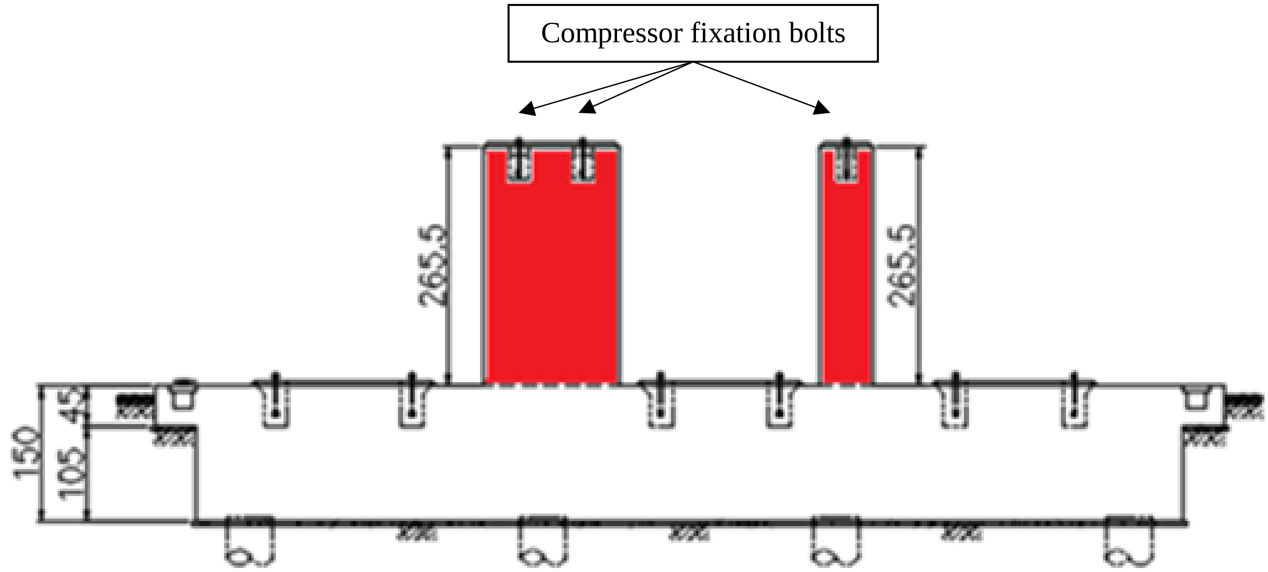

Fig. 5. C-C View from de concrete foundation (dimensions in centimeters).

4. Finite element model

The finite element modeling was developed using ANSYS software, using tridimensional solid hexahedral elements with eight nodes and three degrees of freedom per node, each associated with the translational displacements on the three Cartesian axes. The concrete piles and the soil were modeled with linear spring elements, each with stiffness associated with the translational displacements (X, Y, Z) referring to the concrete piles and soil stiffness. Table 1 presents all input data for the material models and it is important to highlight that ANSYS software was set to perform linear elastic analyses. The structure model resulted in a mesh with 8876 nodes and 6590 elements, totaling 26588 degrees of freedom. Figures 6 and 7 present the finite element model developed in this study. The model was restrained at the free end of the springs (no displacement) and had all of its edges and sides without restraining.

Table 1
Physical Properties of Soil, Concrete Piles and Concrete Block.

Physical Properties	Numerical Value	Constituive Model
Soil Stiffness (kN/m)	20000	Isotropic Linear Elastic – Spring X Direction
Concrete Pile Stiffness (kN/m)	500000	Isotropic Linear Elastic – Spring Y Direction
Soil Stiffness (kN/m)	20000	Isotropic Linear Elastic – Spring Z Direction
Concrete Block Young's Modulus (GPa)	26	Isotropic Linear Elastic
Poisson's Ratio	0.2	-
Density (kg/m³)	2548.42	-

Two dynamic analyses were developed with the finite element model. The first, a modal analysis, consists in the free vibration analysis, which solves the eigenvalues and eigenvectors problem associated with the free vibration condition of the structure. For that, the first ten vibration modes of the structure were extracted. In the second analysis, a forced vibration study of the concrete foundation was developed.

The structure supports a motor-driven compressor which operates with deterministic cyclic loadings, so that forced vibration analysis was developed based on a harmonic sinusoidal loading, simulating the rotary unbalance from the machinery. Table 2 presents equipment data from which it was possible to establish the amplitude of the sinusoidal force as well as its operating frequency.

It is important to highlight that the sinusoidal loading from the equipment acts in all directions of the YZ plane, with components in the Y and Z directions, such that when the loading reaches its maximum amplitude in the Z direction, its value is zero in the Y direction and vice versa. In this way, there are two sinusoidal loadings that are out of phase by 90 degrees. Therefore, the rotary unbalance induces loadings in all directions of the YZ plane given by the vector sum of the Y and Z components in every time instant. Figures 8 and 9 present graphs illustrating the behavior of the Y and Z components of the sinusoidal loadings.

Thus, the dynamic loadings were modeled from sinusoidal loadings with the amplitudes and frequencies of each piece of equipment and applied to the nodes representing the points of the fixation bolts of the equipment, represented by the nodes A to J for the engine, and K to O for the compressor (Figure 10).

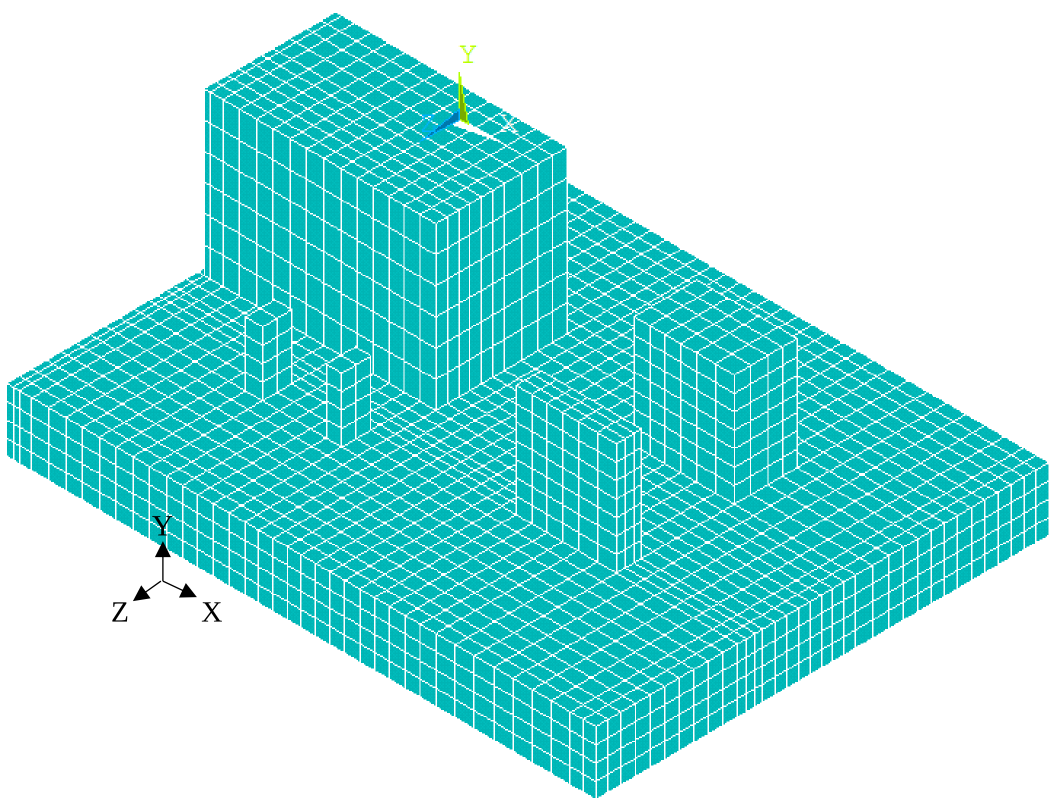

Fig. 6. Structural finite element model.

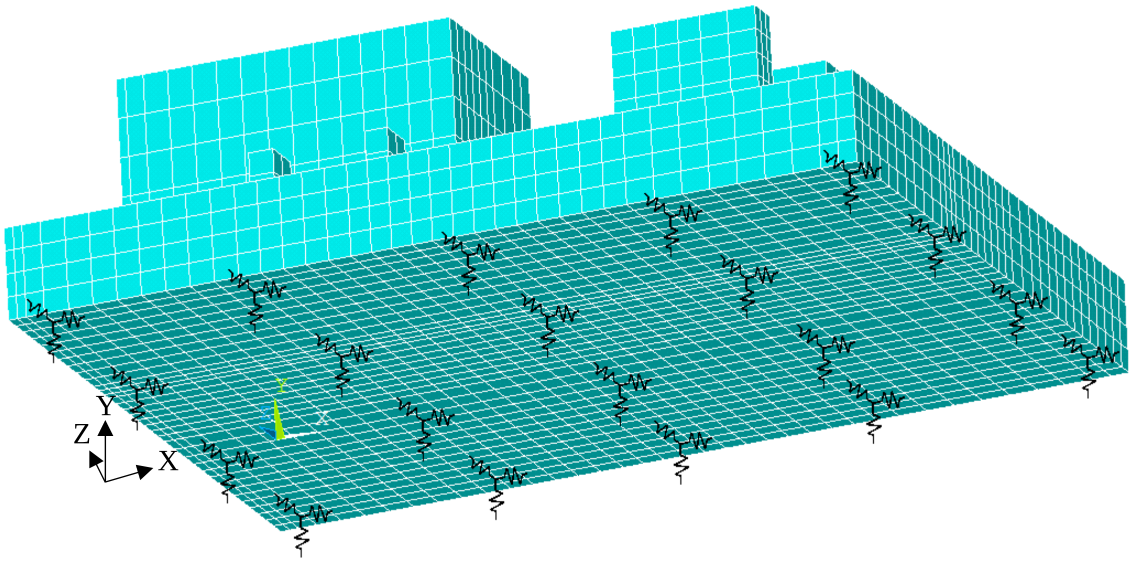

Fig. 7. Linear springs elements (Concrete piles and soil stiffness).

Table 2
Equipment loading data.

Equipment	Operating frequency	Force Amplitude
Engine	188.49 rad/s (30 Hz)	8.5 kN
Compressor	188.49 rad/s (30 Hz)	6.3 kN

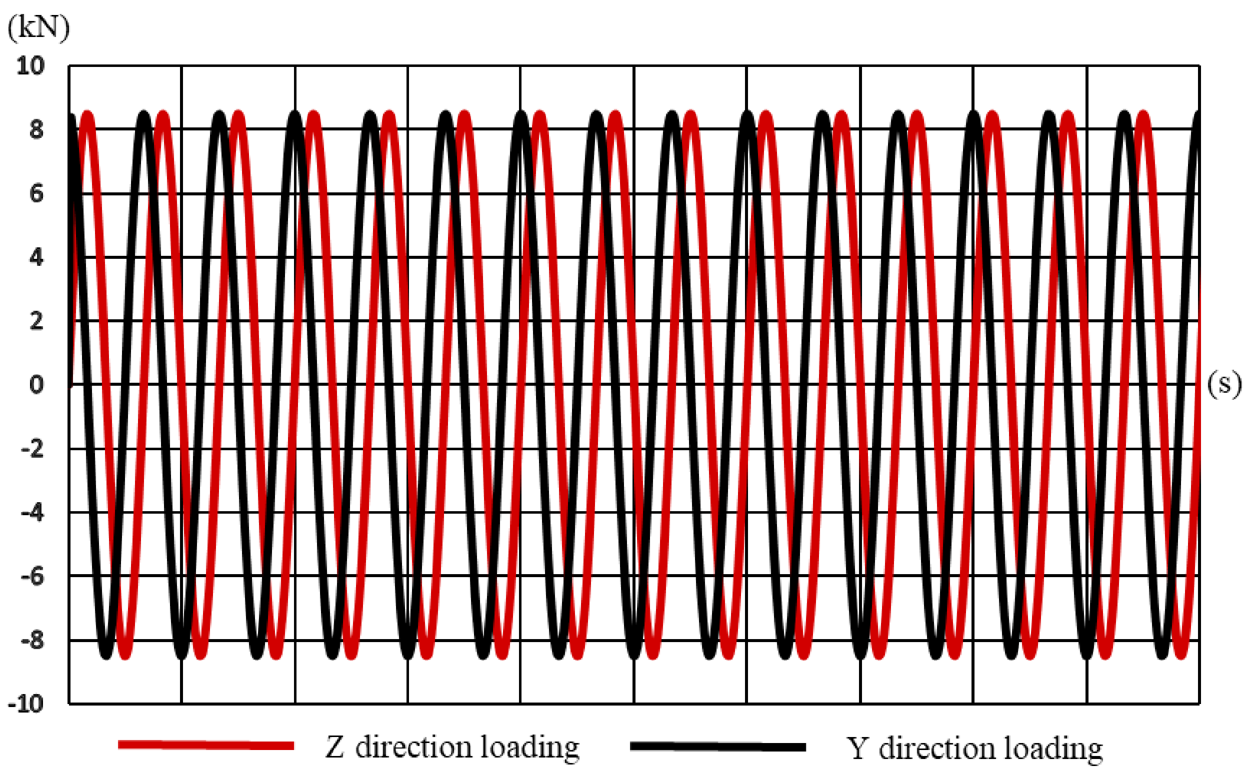

Fig. 8. Engine dynamic loading graph.

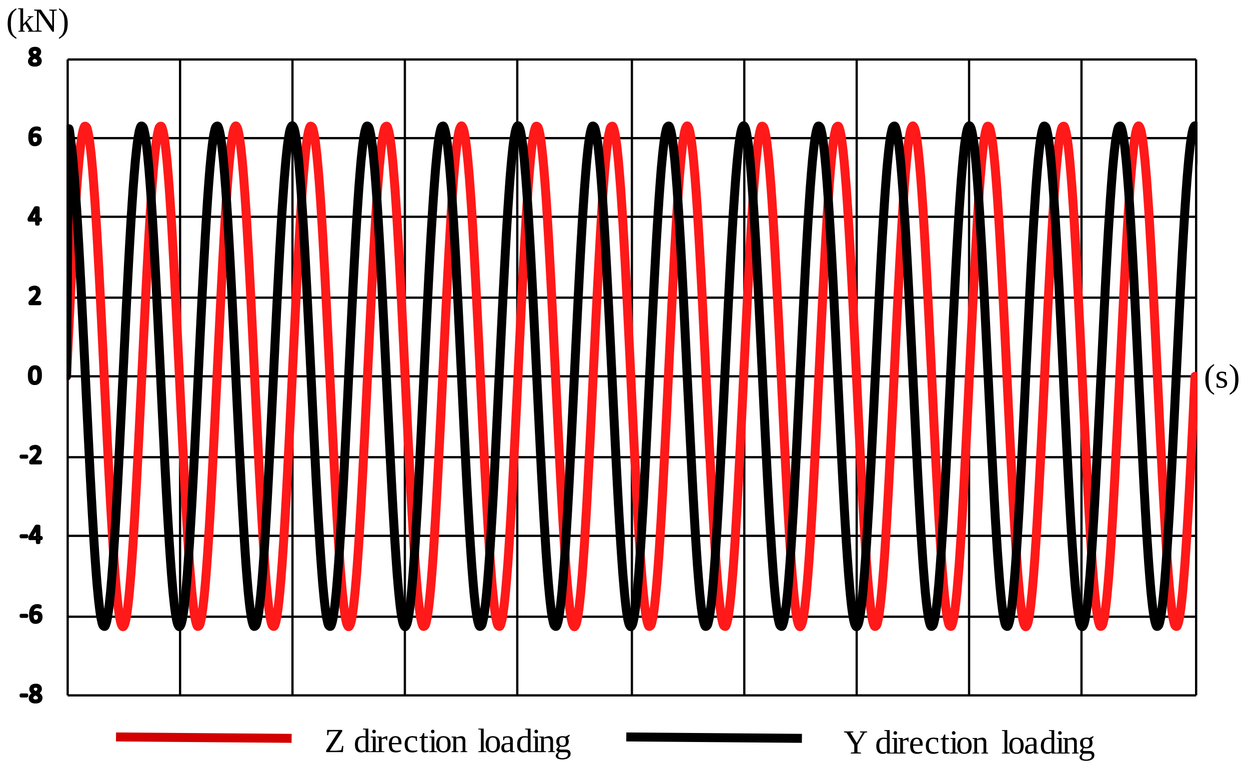

Fig. 9. Compressor dynamic loading graph.

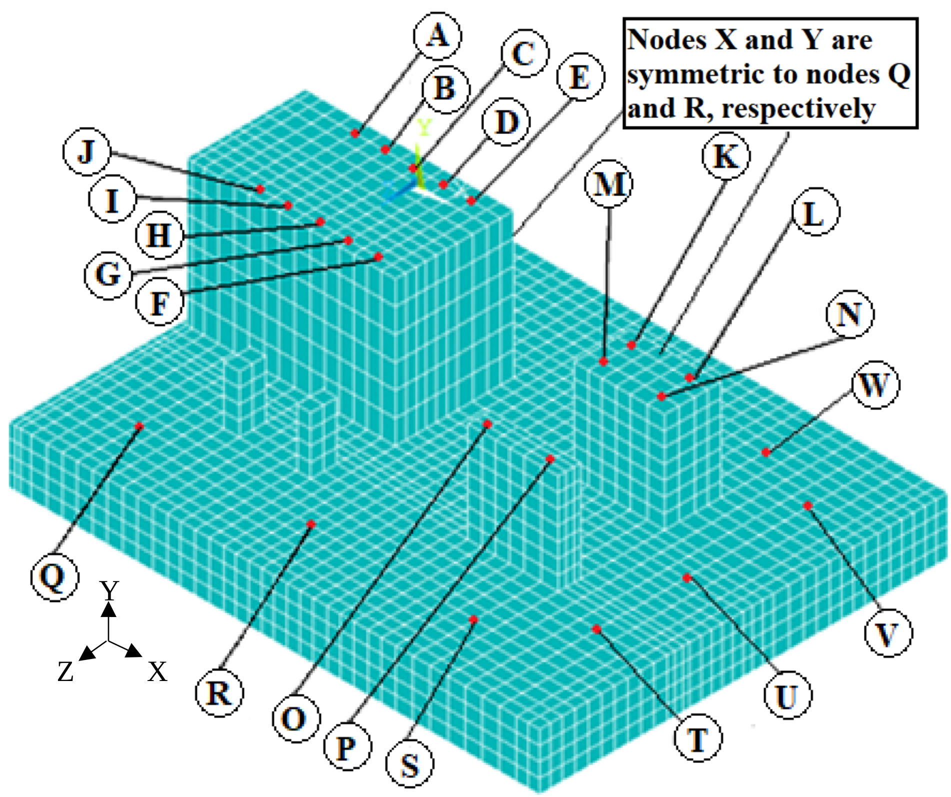

Fig. 10. Selected nodes.

5. Dynamic analyses

Table 3 presents the natural frequencies associated with the first ten vibration modes of the structure, and it is possible to observe the model's deformed shape for some of these vibration modes in Figures 11 to 15. The first and fourth vibration modes represent a translation in X axis direction (Figures 11 and 13); the third represents a rotation in Y axis direction (Figure 12); the fifth represents a bending in Z axis direction (Figure 14) and the sixth represents a bending in X direction (Figure 15).

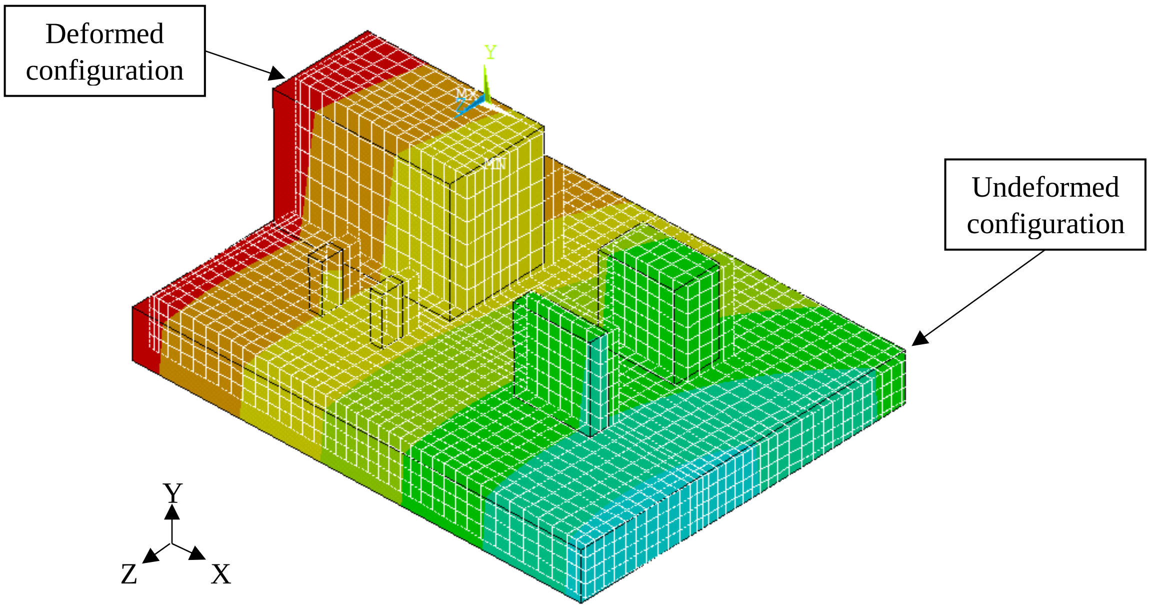

Fig. 11. First vibration mode – f_{01} = 3.46 Hz (Translation in X direction).

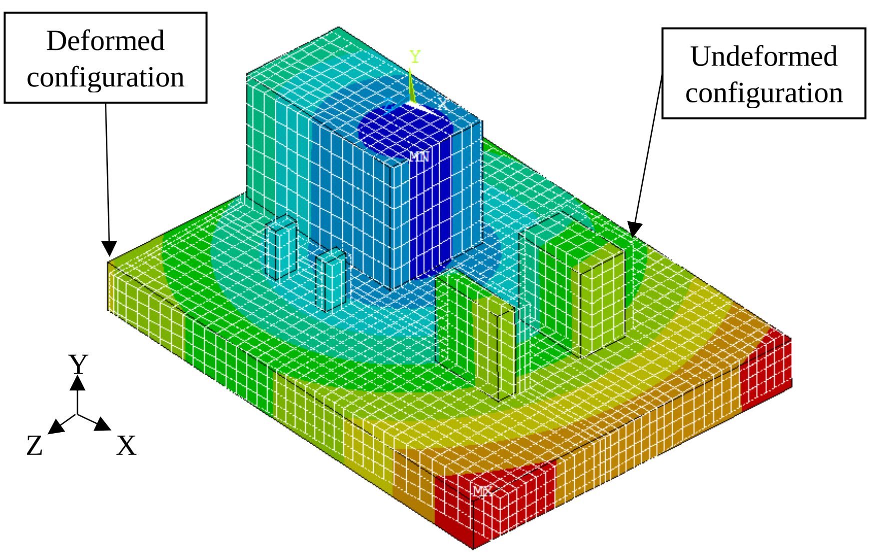

Fig. 12. Third vibration mode – f_{03} = 4.35 Hz (Rotation in Y direction).

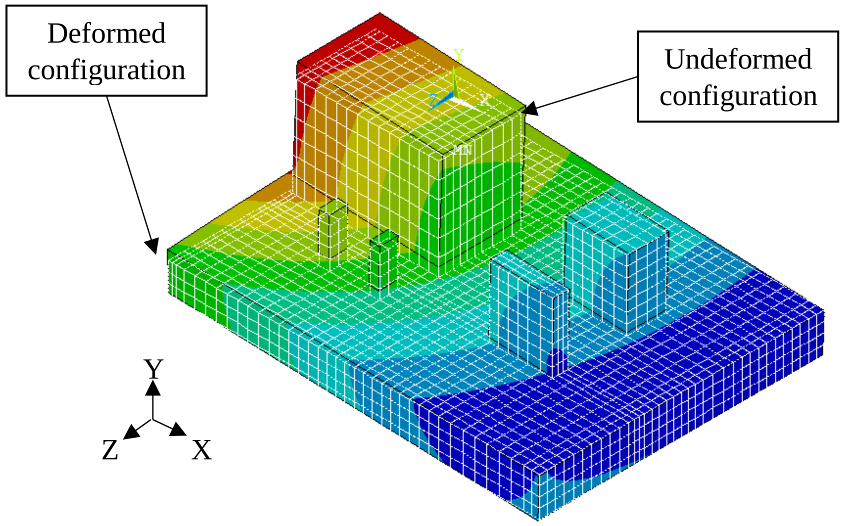

Fig. 13. Fourth vibration mode – f_{04} = 15.49 Hz (Translation in X direction).

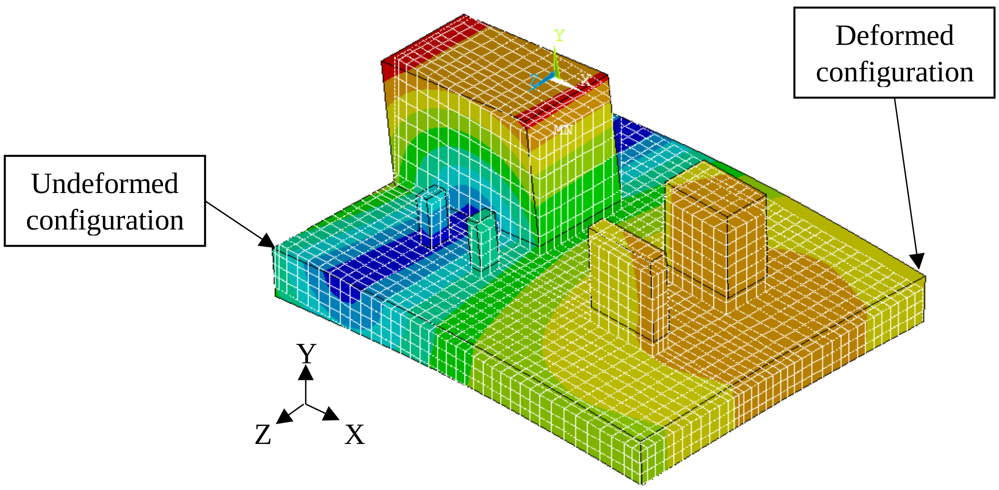

Fig. 14. Fifth vibration mode – f_{05} = 18.09 Hz (Bending in Z direction).

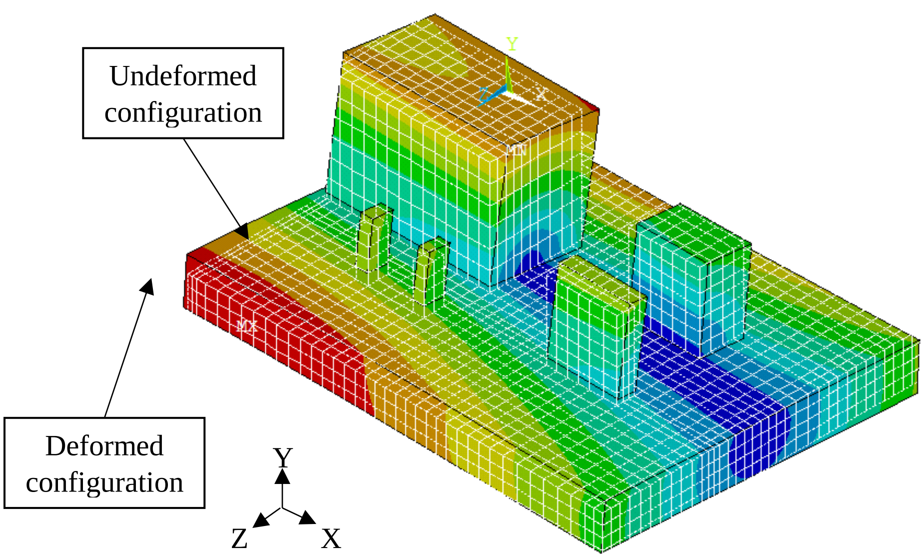

Fig. 15. Sixth vibration mode – f_{06} = 19.49 Hz (Bending in X direction).

The forced vibration analysis led to results in terms of maximum displacements and velocities evaluated at nodes A to J and K to O (Figure 10) and its results are listed also in Table 3. From these results, it is possible to observe that node L presents the higher displacements and velocities (5.1 μm and 0.99 mm/s). It is important to highlight the fact that all data shown in Table 3 are in absolute values, which means that it does not matter whether the displacements and velocities are in the negative or the positive direction along the Y axis.

Accelerations were analyzed at a total of nine points of the structure (represented by nodes Q to Y in Figure 10), chosen in an area of the foundation which has a region of human transit, with the focus on evaluating the conditions of human comfort and safety of people working at the place. Table 3 also presents the maximum absolute values (with no concern about the orientation of the movement) for these accelerations. It is possible to observe that nodes S, V, and W present the higher values of accelerations of about 0.30 m/s².

Table 3
Maximum displacements, velocities, accelerations and natural frequencies.

Nodes	Maximum Displacements (μm)	Maximum Velocities (mm/s)	Nodes	Maximum Accelerations (m/s²)	Vibration Modes	Associated Natural Frequencies (Hz)
A	3.81	0.48	Q	0.21	1	3.46
B	3.53	0.48	R	0.24	2	3.55
C	3.35	0.48	S	0.32	3	4.35
D	3.42	0.47	T	0.24	4	15.49
E	3.56	0.51	U	0.15	5	18.09
F	3.91	0.51	V	0.34	6	19.49
G	3.80	0.51	W	0.36	7	26.13
H	3.71	0.51	X	0.14	8	28.90
I	3.77	0.60	Y	0.15	9	37.67
J	4.00	0.65	-	-	10	44.46
K	4.42	0.69	-	-	-	-
L	5.10	0.99	-	-	-	-
M	3.60	0.75	-	-	-	-
N	4.38	0.89	-	-	-	-
O	3.82	0.66	-	-	-	-
P	4.06	0.78	-	-	-	-

6. Structural optimization

The original design of the concrete foundation has a volume of 310.70 m³. Two optimization analyses were developed using the GA with 20 generations with 90 individuals each. The analyses differ in terms of the crossover and mutation rates used. In the first one, the crossover and mutation rates were fixed at 70% and 10%, respectively, while in the second analysis these rates varied along the generations, with initial crossover and mutation rates of 70% and 10% and final ones of 50% and 30%. There are no recommended practical values for number of individuals, generations, and crossover and mutation rates. In other hand, the mutation rate should be low, in order to preserv the genetic data from the individuals, but sufficient to prevent the GA from meeting a local minimum. It is important to use values for such parameters that best suit the proposed optimization problem, observing the behavior of the GA in the search for the optimal solution. In other words, the GA user should try some differents parameters for number of individuals and generations and evaluate the behavior of the GA.

After the application of GA to the problem, the first analysis led to a configuration with a volume of 157.00 m³, which represents a 49.40% reduction from the original configuration. In the second analysis, the final volume was 157.30 m³, representing a volume reduction of about 49.30%. Table 4 presents the optimum dimensions compared with the original ones.

Table 4
Dimensions of the concrete foundation.

Design Variable	**Original**	**Optimum** (First Analisys)	**Difference**	**Optimum** (Second Analisys)	**Optimum**
x_1	1.500 m	0.70 m	53.33%	0.70 m	53.33%
x_2	3.838 m	2.25 m	41.38%	2.31 m	39.81%
x_3	2.655 m	1.95 m	26.55%	1.79 m	32.58%

For the natural frequencies of the optimum design configurations, Tables 5 presents the values of the six first vibration modes in comparison to the original configuration values and with the 10% minimum difference constraint with respect to the equipment excitation frequency (30 Hz), as estabilished by DIN 4024 standard [18,19].

The maximum displacements and velocities obtained by dynamic analyses of the optimum design configurations can be observed in Tables 6 and 7 in comparison with the original configuration values. Tables 6 and 7 also show the maximum displacements and velocities limits (from ISO 2372 standard recommendations [20]) used as the optimization constraints.

Table 5
Natural frequencies for the first and second optimization analyses.

f_n	**Original (Hz)**	**Optimum - First Analysis (Hz)**	**Difference - First Analysis**	**Constraint (% 30 Hz) - First Analysis**	**Optimum - Second Analysis (Hz)**	**Difference - Second Analysis**	**Constraint (% 30 Hz) - Second Analysis**
1	3.46	4.84	39.90%	-0.74	4.84	39.90%	-0.74
2	3.55	5.00	40.80%	-0.73	5.00	40.80%	-0.73
3	4.35	6.23	43.20%	-0.69	6.25	43.60%	-0.69
4	15.49	19.36	25.00%	-0.25	19.23	24.20%	-0.26
5	18.09	22.40	23.80%	-0.15	22.38	23.70%	-0.15
6	19.49	26.83	37.70%	-0.01	26.68	36.90%	-0.01

Table 6
Displacements for the first and second optimization analyses.

Nodes	Original (µm)	Optimum (µm) - First Analysis	Difference - First Analysis	Constraint (Maximum 20 µm) - First Analysis	Optimum (µm) - Second Analysis	Difference - Second Analysis	Constraint (Maximum 20 µm) - Second Analysis
A	3.81	15.46	306%	-4.54	14.10	270%	-5.90
B	3.53	14.11	300%	-5.89	12.43	252%	-7.57
C	3.35	12.79	282%	-7.21	11.89	255%	-8.11
D	3.42	13.25	287%	-6.76	12.90	277%	-7.1
E	3.56	14.40	304%	-5.60	14.29	301%	-5.71
F	3.91	11.87	204%	-8.13	11.18	186%	-8.82
G	3.80	12.36	225%	-7.64	11.53	203%	-8.47
H	3.71	12.87	247%	-7.13	11.89	220%	-8.11
I	3.77	13.38	255%	-6.62	12.23	224%	-7.77
J	4.00	14.56	264%	-5.44	13.73	243%	-6.27
K	4.42	10.63	140%	-9.37	10.63	141%	-9.37
L	5.10	15.74	209%	-4.26	16.52	224%	-3.48
M	3.60	9.84	173%	-10.16	10.99	205%	-9.01
N	4.38	14.65	234%	-5.35	16.61	279%	-3.39
O	3.82	11.12	191%	-8.88	11.72	207%	-8.28
P	4.06	13.85	241%	-6.15	14.84	265%	-5.16

In terms of accelerations, the dynamic analyses of the optimum designs led to the results listed in Table 8. These acceleration values are compared with the original design configuration and with the limits of the human comfort constraint established by the ISO 2631 standard [21,22].

Table 7
Velocities for the first and second optimization analyses.

Nodes	Original (mm/s)	Optimum (mm/s) - First Analysis	Difference - First Analysis	Constraint (Maximum 2.8 mm/s) - First Analysis	Optimum (mm/s) - Second Analysis	Difference - Second Analysis	Constraint (Maximum 2.8 mm/s) - Second Analysis
A	0.48	2.56	433%	-0.24	2.21	361%	-0.59
B	0.48	2.27	374%	-0.53	2.00	316%	-0.80
C	0.48	2.14	347%	-0.66	1.95	306%	-0.85
D	0.47	2.18	363%	-0.62	2.12	351%	-0.68
E	0.51	2.40	370%	-0.40	2.39	368%	-0.41
F	0.51	2.08	308%	-0.72	1.91	274%	-0.89
G	0.51	2.10	311%	-0.70	1.94	280%	-0.86
H	0.51	2.13	317%	-0.67	1.97	287%	-0.83
I	0.60	2.15	259%	-0.65	2.01	234%	-0.79
J	0.65	2.34	260%	-0.46	2.13	2,28	-0.67
K	0.69	1.85	169%	-0.95	1.77	157%	-1.03
L	0.99	2.79	182%	-0.01	2.79	182%	-0.01
M	0.75	1.61	115%	-1.19	1.83	144%	-0.97
N	0.89	2.49	180%	-0.31	2.77	211%	-0.03
O	0.66	2.05	210%	-0.75	1.90	188%	-0.90
P	0.78	2.59	232%	-0.21	2.77	255%	-0.03

Table 8
Accelerations for the first and second optimization analyses.

Nodes	Original (m/s^2)	Optimum (m/s^2) - First Analysis	Difference - First Analysis	Constraint (1.0 m/s^2) - First Analysis	Optimum (m/s^2) - Second Analysis	Difference - Second Analysis	Constraint (1.0 m/s^2) - Second Analysis
Q	0.21	0.74	254%	-0.26	0.67	217%	-0.33
R	0.24	0.62	157%	-0.38	0.58	143%	-0.42
S	0.32	0.55	72%	-0.45	0.50	57%	-0.50
T	0.24	0.60	150%	-0.40	0.61	156%	-0.39
U	0.15	0.59	291%	-0.41	0.63	323%	-0.37
V	0.34	0.68	101%	-0.32	0.68	99%	-0.32
W	0.36	0.55	52%	-0.45	0.52	45%	-0.48
X	0.14	0.56	297%	-0.44	0.59	325%	-0.41
Y	0.15	0.71	373%	-0.29	0.64	326%	-0.36

Tables 6 and 8 present the displacements and acceleration constraints and it is important to notice that these values still are below their limits (estabilished by ISO 2372 and ISO 2631) [20–22] with a considerable difference for both designs proposed by the two optimization analyses. On the other hand, from the maximum velocities obtained for the first optimization analysis design (Table 7), it is possible to see that the value of the velocity at node L is close to that established by the ISO 2372 standard [20], namely 2.8 mm/s. Table 7 also presents the maximum velocities for the second optimization analysis design; for the nodes L, N, and P, those velocities were very close to the limits [20]. Regarding the natural frequencies constraints, it can be seen that the values referring to the first six vibration modes all meet the minimum difference of 10% relative to the equipment excitation frequency (30 Hz), as estabilished by DIN 4024 standard [18,19].

All constraints used for optimization were based on criteria from ISO 2372 [20], DIN 4024 [18,19] and ISO 2631[21,22] standards, as represented by Eqs. 2 to 5. It is important to note that from the values presented in Tables 5, 6, 7 and 8 for both optimization analyses, constraints are being respected. From this observation, it can be concluded that the safety of the concrete foundation has not been modified by optimization.

Figures 16 and 17 present the GA's evolution along the generations with the values of the objective function to the best individual and the mean value of the objective function for the individuals of each generation. The behavior of the GA was practically the same for the two analyses. The higher volume reduction was obtained for the first generations and little volume reductions were achieved for the following ones.

Considering the behavior presented by the GA during the two optimization analyses, it is possible to verify that in the first generations the structural volume reduction corresponds to approximately 90% of the total volume reduction over the 20 generations. Such behavior indicates that early in the first generations the GA encountered an individual that was much fitter than that considered for the original design configuration. At the end of the generations, the volume reduction is not very significant when compared to the reduction that occurs in the first generations; however, it should be emphasized that the volume reduction of the structure (in its optimum design configuration) is quite considerable when compared to the original volume.

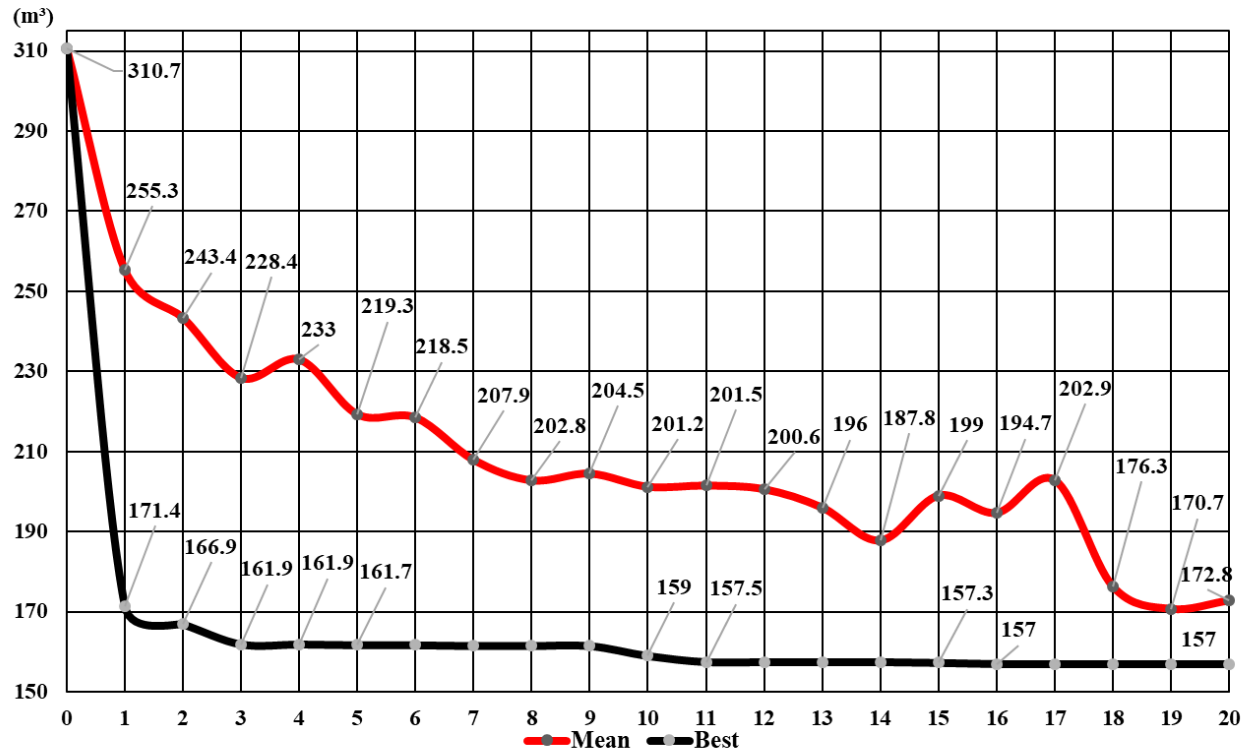

Fig. 16. Evolution of the GA in the first analysis.

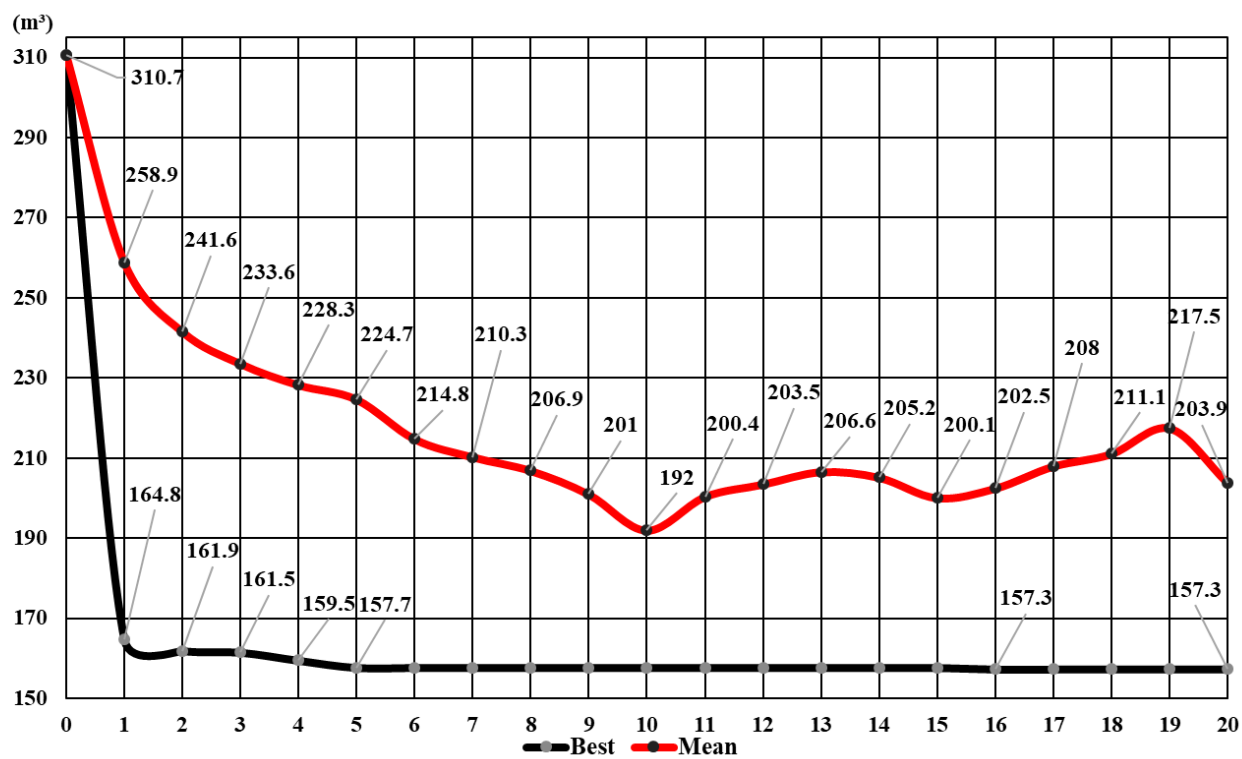

Fig. 17. Evolution of the GA in the second analysis.

In terms of a comparison between the two optimization analyses performed, no advantages of using variable rates of crossover and mutation along the generations were observed. Comparing the graphs in Figures 16 and 17, it was observed that in the first analysis, the value of the mean objective function for the individuals along the generations tended to approach the optimum value; that is, the population was found to be increasingly fit and the individuals had more similar characteristics. In the second analysis, it was verified that the mean of the objective function of the individuals was unstable from the 10th generation onwards, increased until the 13th generation, then decreased until the 15th, increased again until the 19th, and once again decreased in the 20th. Such instability is justified by the increase in mutation rates, increasing the diversification of the population that makes up the next generation.

With regard to the evolution of the GA, it was noticed that, for the two analyses performed, the search for the fittest individual occurred in a similar way, as an individual that would achieve the design in a much more economical way than the original configuration was already found in the first generation and the optimum individual was obtained from the 16th generation onward.

7. Conclusion

The main focus of this study was to develop a structural optimization model of a concrete foundation designed to support a high-capacity motor-driven compressor with a dynamic analysis of the structure aiming to predict its behavior and to constrain its displacements, velocities, accelerations, and natural frequencies in the optimization analyses. For that, a Genetic Algorithm (GA) was applied to the problem using the MATLAB-ANSYS interface in order to obtain the best structural volume reduction possible without compromising the functioning of the equipment, the safety of people, and the design recommendations.

For the natural frequencies constraints, the six first vibration modes of the structural system were considered according to the design recommendations set out by the DIN-4024 standard. The values obtained for those vibration modes in both optimum design configurations attained a minimum difference of 10% relative to the equipment excitation frequency (30 Hz), as per the standard recommendation.

Regarding the constraints, the maximum displacements (Maximum displacement = 16.61 μm < Constraint Limit = 20 μm) and acceleration (Maximum acceleration = 0.74 m/s^2 < Constraint Limit = 1.0 m/s^2) limits set by the standards have been met with a certain considerable difference. As for the maximum velocity (Maximum velocity = 2.79 mm/s < Constraint Limit = 2.8 mm/s) limits imposed on the structure in its two optimum design configurations, the values were very close to those established by the standards, so this was the most important constraint to limit the structural optimization.

From the two optimization analyses it was found that the percentage volume reduction was about 49.40%, reducing the structural volume from 310.7 to 157 m^3 in the first analysis and to 157.30 m^3 in the second one. Considering a mean cost of 250.00 BRL (Brazilian reals) per cubic meter of concrete, it is possible to verify savings of 38000.00 BRL per foundation of 76000.00 BRL for both foundations.

References

[1] Lopes MA. Structural optimization of a concrete foundation subjected to dynamic loadings from a high capacity motor-driven compressor. Master's dissertation (Mechanical Engineering Master's Degree) – Mechanical Engineering Postgraduate Program (PPGEM), State Univer. 2017.

[2] Lopes MA, Soeiro FJCP, Burgos RB. Structural optimization of a concrete foundation subjected to dynamic loadings from a motor-compressor group. XXXVIII Iber Lat Am Congr Comput Methods Eng (CILAMCE), Florianopolis/SC, Brazil 2017.

[3] Lopes DMC. Numerical analysis and study of dynamic response of structural systems for machinery foundations. 1f. Master's dissertation (Civil Engineering Master's Degree) - Civil Engineering Postgraduate Program (PGECIV), State University of Rio de Janeiro (UERJ), R. 2016.

[4] Holland J. An introduction with application to biology, control and artificial intelligence Adaptation in Natural and Artificial System 1975.

[5] Adeli H, Cheng N. Augmented Lagrangian Genetic Algorithm for Structural Optimization. J Aerosp Eng 1994;7:104–18. doi:10.1061/(ASCE)0893-1321(1994)7:1(104).

[6] Tan LP, Lotfi A, Lai E, Hull JB. Soft computing applications in dynamic model identification of polymer extrusion process. Appl Soft Comput 2004;4:345–55. doi:10.1016/j.asoc.2003.10.004.

[7] Grierson DE, Hajela P. Emergent computing methods in engineering design: applications of genetic algorithms and neural networks. vol. 149. Springer Science & Business Media; 1996.

[8] Prendes Gero MB, Bello García A, del Coz Díaz JJ. A modified elitist genetic algorithm applied to the design optimization of complex steel structures. J Constr Steel Res 2005;61:265–80. doi:10.1016/j.jcsr.2004.07.007.

[9] Tayşi N, Göğüş MT, Özakça M. Optimization of arches using genetic algorithm. Comput Optim Appl 2008;41:377–94. doi:10.1007/s10589-007-9111-3.

[10] Vasudev KL, Sharma R, Bhattacharyya SK. Multi-objective shape optimization of submarine hull using genetic algorithm integrated with computational fluid dynamics. Proc Inst Mech Eng Part M J Eng Marit Environ 2019;233:55–66. doi:10.1177/1475090217714649.

[11] Rajeev S, Krishnamoorthy CS. Discrete Optimization of Structures Using Genetic Algorithms. J Struct Eng 1992;118:1233–50. doi:10.1061/(ASCE)0733-9445(1992)118:5(1233).

[12] Hajela P, Lee E. Genetic algorithms in truss topological optimization. Int J Solids Struct 1995;32:3341–57. doi:10.1016/0020-7683(94)00306-H.

[13] Camp C, Pezeshk S, Cao G. Optimized Design of Two-Dimensional Structures Using a Genetic Algorithm. J Struct Eng 1998;124:551–9. doi:10.1061/(ASCE)0733-9445(1998)124:5(551).

[14] Hosseini G. Capacity Prediction of RC Beams Strengthened with FRP by Artificial Neural Networks Based on Genetic Algorithm. J Soft Comput Civ Eng 2017;1:93–8.

[15] Olivier LT, Jimoh AA, Adedeji AA. Optimisation of Recycled Thermoplastic Plate (Tile). J Soft Comput Civ Eng 2017;1:19–34.

[16] Karanjule DB, Bhamare SS, Rao TH. Process Parameter Optimization for Minimizing Springback in Cold Drawing Process of Seamless Tubes using Advanced Optimization Algorithms. J Soft Comput Civ Eng 2018;2:72–90.

[17] American Concrete Institute. "ACI 351 – Foundations for Dynamic Equipment." Farmington Hills, Michigan, United States of America, 2004.

[18] Deutsches Institut Für Normung. "DIN 4024-1 – Machine Foundations – Rigid Foundations for Machinery Subjected to Periodic Vibration", Berlin, German, 1998.

[19] Deutsches Institut Für Normung. “DIN 4024-2 – Machine Foundations – Rigid Foundations for Machinery Subjected to Periodic Vibration.” Berlin, German, 1991.

[20] International Standard Organization. “ISO 2372: Mechanical Vibration of Machines with Operating Speeds from 10 to 200 rev/s.” Basis for Specifying Evaluation Standards., n.d.

[21] International Standard Organization. ISO 2631-1: “Mechanical Vibration and Shock - Evaluation of Human Exposure to Whole-Body Vibration – Part 1: General Requirements.,” 1997.

[22] International Standard Organization. ISO 2631-2: “Evaluation of Human Exposure to Whole-Body Vibration – Part 2: Human Exposure to Continuous and Shock-Induced Vibrations in Buildings (1 to 80Hz).,” 2001.

[23] Norma Regulamentadora. NR 15. Attachment N° 8: Vibrations – Amended by Ordinance SSMT N. ° 12, Ministry of Labour, Brazil., 1983.

[24] Petrobras – Petróleo Brasileiro S.A. – “N-1848 – REV. C – Design of Machine Foundation” Rio de Janeiro, Brazil., 2011.